An Optimized High-Order Implicit FDTD Solver with One-Sided TF/SF for Simulation of Photonic Devices

Hossam A Abdallah
The George Washington University, Washington DC-USA

Abstract: In this paper an optimized high-order implicit finite difference time domain (FDTD) solver with one-sided total-field/scattered-field (TF/SF) excitation is developed for numerical simulation of integrated optical components. The optimized FDTD algorithm reduces the number of operations and the storage requirements to perform the matrix inversion using LU decomposition. It is shown that the one-sided TF/SF formulation is more accurate in launching the exact power into the simulation domain as well as decreasing the load on the PML-ABCs. The implementation of this tool was done in the Prometheus program, a software package of Kymata Netherlands.

Keywords: FDTD, TF/SF, Photonic devices

1. Introduction

There are different wave modeling techniques that are successfully used in modeling integrated optical structures. Finite difference time domain (FDTD), Fourier transform-beam propagation method (FT-BPM), finite difference-beam propagation method (FD-BPM), and finite element beam propagation method (FE-BPM) are the most popular and useful techniques for the simulation of integrated optics structures. FT-BPM, FD-BPM, and FE-BPM were developed for the case of weakly guiding structures where the use of the paraxial approximation and the neglection of any back reflections offer solutions in the frequency-domain. These characteristics limited the use of these methods when these assumptions are no longer valid.

The FDTD method overcomes the disadvantages of the previous methods. In simulating guided-wave optics the method became increasingly popular due to its attractive features such as ease of implementation and full-wave simulation including multiple reflections and radiation. The first FDTD algorithm proposed by Yee [1] provides a simple and a direct solution to the Maxwell's equations. However, the Yee FDTD scheme that is second order in both space and time, we refer to it as Yee(2,2), is dispersive, less accurate, and computational expensive. Higher-order FDTD schemes [2] overcome these problems but come at a higher computational cost. In this paper we implemented an implicit fourth order scheme in space and second order in time [3], we refer to it as Implicit(2,4). The Implicit(2,4) scheme introduces substantial accuracy and improvement over Yee(2,2) and because it is unconditional stable arbitrary time steps can be chosen. Detail analysis of the dispersion and accuracy of the Yee(2,2) and Implicit(2,4) schemes were performed in 1D and the results in [4]. The Implicit(2,4) algorithm requires the inversion of a tridiagonal matrix, which can be replaced by decomposing the matrix using the LU decomposition. We derive a simple algorithm to perform the LU decomposition. The new algorithm reduces the number of operations and the storage requirements to perform the LU decomposition.

It is known that implementation of sources in FDTD simulations requires more complicated procedures. The complications come from the requirements to terminate waveguides that are extended beyond the grid boundaries. All excitation techniques intend to couple the exact incident power to the FDTD grid, allow back reflected waves to pass through the excitation position, to avoid the interaction between simulated sources and the absorbing boundary conditions (ABCs), and, finally, to decrease the load on the ABCs. A popular method is the use of the total-field/scattered-field (TF/SF) method [5]. By introducing the TF/SF formulation, the simulation domain will be divided into three domains: the total-field domain, the scattered field domain, and the ABCs domain (we use the perfectly matching layer PML ABCs in all our simulations). The SF domain offers information about any scattered field meanwhile decreasing the load on ABCs.

In most of the structures of interest to our work the amount of scattering on the right side of the simulation domain is much less compared to the left side and therefore no scattered field region is added on the right side of the simulation domain. We refer to such formulation the one-sided TF/SF formulation. Implementation as well as illustrative example of the one-sided TF/SF formulation is described in detail in Section 3.

Finally the developed simulation tool was used to analyze a number of structures that are excited by waveguides. The accuracy of the results was compared to the accuracy of the Prometheus program (a beam propagation based solver).

This paper is organized into four sections as follow. Following this Introduction Section, Section 2 introduces the optimized LU decomposition of the Implicit(2,4) FDTD scheme. Section 3 introduces the one-sided TF/SF formulation and some simulation results obtained using this formulation together with the Implicit(2,4) FDTD scheme and the PML-ABCs. Finally, Section 4 presents conclusions about the work we presented.

2. Differential Equations and Difference Notations in 1D

In a 2D setting, assuming that both the fields and the dielectric structure are constant along the $y-$direction, Maxwell equations decouple into two sets (we introduce the normalized fields $\tilde{\mathbf{E}}$ and $\tilde{\mathbf{H}}$ as $\tilde{\mathbf{E}} = \sqrt{\varepsilon_0/\mu_0}\,\mathbf{E}$, $\tilde{\mathbf{H}} = \mathbf{H}$, with the speed of light in free space $c_0 = 1/\sqrt{\varepsilon_0\mu_0}$, and we drop the hat above the normalized fields) One set is constituted by electromagnetic fields with vanishing components $E_x,\ E_z,\ H_y$.

$$\varepsilon_r \partial_t E_y = c_0\left(\partial_z H_x - \partial_x H_z\right), \tag{1}$$

$$\partial_t H_x = c_0 \partial_z E_y, \tag{2}$$

$$\partial_t H_z = -c_0 \partial_x E_y. \tag{3}$$

These fields are called the TE fields. The second set has vanishing $E_y,\ H_x,\ H_z$ components.

$$\partial_t H_y = -c_0\left(\partial_z E_x - \partial_x E_z\right), \tag{4}$$

$$\varepsilon_r \partial_t E_x = -c_0 \partial_z H_y, \tag{5}$$

$$\varepsilon_r \partial_t E_z = c_0 \partial_x H_y. \tag{6}$$

These fields are called TM fields. The two sets are completely decoupled; there is no common field vector component. Therefore TE and TM fields constitute two possible classes of solutions for two-dimensional electromagnetic problems. If the medium is inhomogeneous along the x-direction, then boundary conditions at material interfaces imply that E_y, $\frac{\partial E_y}{\partial x}$, and H_z are continuous for TE fields. For TM fields H_y and E_z are continuous while $\frac{\partial H_y}{\partial x}$ is not.

We introduce and derive some notations for the finite differences that will be used for the FDTD schemes under consideration. For simplicity we consider a one dimensional finite difference notation. We apply and analyze different FDTD schemes in $1\mathbf{D}$ and then extend the implementation of the most appropriate scheme to $2\mathbf{D}$. The TE field equations in $1\mathbf{D}$ are

$$\varepsilon_r \partial_t E_y = c_0 \partial_z H_x, \tag{7}$$

$$\partial_t H_x = c_0 \partial_z E_y. \tag{8}$$

As shown in Figure 1 and as proposed by Yee [1], the discretization points for E_y and H_y are interleaved in space and time. We present notations for approximating the first and second derivatives in space or time at certain position using the neighboring points. We denote by ζ either E_y or H_x. We assume equidistant discretization with the step size Δz in the z-direction and the time step size Δt and define $\zeta_i^n = \zeta(n\Delta t, i\Delta z)$. δ_z and δ_z^2 are the approximations to the first and second derivative with respect to z, respectively.

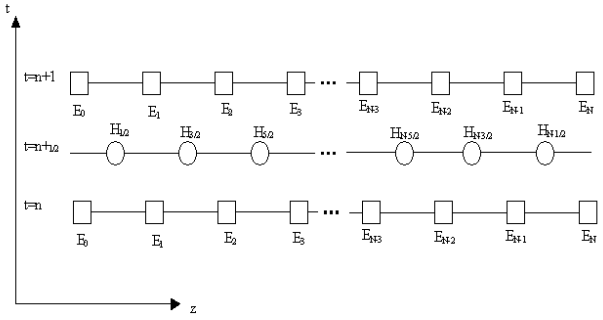

Fig. 1. Position of discretization points in a 1D grid, circles.

We differentiate between two grids. The first grid is the staggered grid in which E_y and H_x are located in space as in Fig. 1, the second grid is the

non-staggered grid in which E_y and Hy are located at the same space and time positions.
For the staggered grid we define the following finite difference expressions

$$\delta_z \zeta_{i+1/2}^n = \frac{\zeta_{i+1}^n - \zeta_i^n}{\Delta z} + O(\Delta z)^2 \quad (9)$$

$$\delta_z \zeta_i^{n+\frac{1}{2}} = \frac{\zeta_{i+1/2}^{n+\frac{1}{2}} - \zeta_{i-1/2}^{n+\frac{1}{2}}}{\Delta z} + O(\Delta z)^2 \quad (10)$$

$$\delta_t \zeta_i^{n+\frac{1}{2}} = \frac{\zeta_i^{n+1} - \zeta_i^n}{\Delta t} + O(\Delta t)^2 \quad (11)$$

$$\delta_t \zeta_{i+\frac{1}{2}}^n = \frac{\zeta_{i+\frac{1}{2}}^{n+\frac{1}{2}} - \zeta_{i+\frac{1}{2}}^{n-\frac{1}{2}}}{\Delta t} + O(\Delta t)^2 . \quad (12)$$

For higher order FDTD schemes we use also the following non-symmetric stencils, for the second order spatial derivatives

$$\delta_z^2 \zeta_{i+1/2}^n = \frac{\zeta_{i-1}^n - 2\zeta_i^n + \zeta_{i+1}^n}{(\Delta z)^2} + O(\Delta z)^2 \quad (13)$$

$$\delta_z^2 \zeta_i^{n+\frac{1}{2}} = \frac{\zeta_{i-3/2}^{n+\frac{1}{2}} - 2\zeta_{i-1/2}^{n+\frac{1}{2}} + \zeta_{i+1/2}^{n+\frac{1}{2}}}{(\Delta z)^2} + O(\Delta z)^2 \quad (14)$$

and for non-staggered grid

$$\delta_z \zeta_i^n = \frac{\zeta_{i+1}^n - \zeta_{i-1}^n}{2\Delta z} + O(\Delta z)^2 \quad (15)$$

$$\delta_t \zeta_i^n = \frac{\zeta_i^{n+1} - \zeta_i^{n-1}}{\Delta t} + O(\Delta t)^2 \quad (16)$$

$$\delta_z^2 \zeta_i^n = \frac{\zeta_{i-1}^n - 2\zeta_i^n + \zeta_{i+1}^n}{(\Delta z)^2} + O(\Delta z)^2 . \quad (17)$$

The minor problem or disadvantage when using staggered grids is the need to perform post-processing calculation/interpolation to evaluate field values at the same spatial and temporal positions. These requirements complicate the simplicity of the FDTD scheme and require additional computation time and programming effort.

2.1 Yee Scheme

Yee formulated the first FDTD scheme [1] on a staggered grid using a second order accurate approximation to the spatial and time derivatives. We will refer to it as Yee(2,2), where (2,2) refers to the order of accuracy in time and space, respectively. For the 1**D** TE fields given by equations (7) and (8), the Yee(2,2) scheme will have the form

$$\varepsilon_r \left| {}_i \delta_t E_y \right|_i^{n+\frac{1}{2}} = c_0 \delta_z H_x \Big|_i^{n+\frac{1}{2}}, \quad (18)$$

$$\delta_t H_x \Big|_{i+\frac{1}{2}}^n = c_0 \delta_z E_y \Big|_{i+\frac{1}{2}}^{n+\frac{1}{2}}. \quad (19)$$

Equations (18) and (19) are rewritten to yield explicit expressions for E_y^{n+1} given $H_x^{n+\frac{1}{2}}$ and E_y^n and for $H_x^{n+\frac{1}{2}}$ given E_y^n and $H_x^{n-\frac{1}{2}}$. Thus, from initial field distribution E_y^0, the algorithm can advance alternatingly E_y and H_x in time. The Yee(2,2) algorithm is a conditionally stable algorithm which means that the time and space steps must satisfy certain criteria. In 1**D** the stability criteria is $\Delta t \le \frac{\Delta z}{c_0}$.

2.2 A Fourth Order Implicit Scheme with Optimized LU Decomposition

In this paper we considered an implicit fourth order scheme in space and second order in time [3]. We refer to it as Implicit(2,4). The derivation of the Implicit(2,4) scheme starts with calculating the truncation error to the fourth order when approximating the first derivatives. This leads to

$$\delta_z \zeta_{i+1/2}^{n+\frac{1}{2}} = (1 + \frac{(\Delta z)^2}{24} \partial_z^2 \Big|_{i+1/2}) \partial_z \zeta_{i+1/2}^{n+\frac{1}{2}} + O(\Delta z)^4 \quad (20)$$

and by introducing a discrete approximation to the operator $\partial_z^2 \Big|_{i+1/2}$ by $\delta^2 \Big|_{i+1/2}$, we obtain

$$\delta_z \zeta_{i+1/2}^{n+\frac{1}{2}} = (1 + \frac{(\Delta z)^2}{24} \delta^2) \frac{\partial \zeta}{\partial z} \Big|_{i+1/2}^{n+\frac{1}{2}} + O(\Delta z)^4 . \quad (21)$$

Demonstrated here for 1D problems, the field values at the grind points are calculated in two steps. In the first step the values of the first order derivatives are calculated directly from the difference equation and in the second step these derivatives are expressed explicitly in terms of the field values of the neighboring grid points. The second step involves the inversion of a matrix, which is tridiagonal except at the first and last rows (this because of the need to use one sided

fourth order accurate implicit approximations to the derivatives at the first and last points at the boundary). In 2D and 3D the spatial derivatives are approximated in the same way and the matrices that relate the fields with their derivatives will be the same.

The inversion of the tridiagonal matrix can be replaced by decomposing the matrix using the LU decomposition. Performing the LU decomposition requires 5N operations and L and U will be bidiagonal matrices, except at a few rows, with one of them containing ones on the diagonal [3]. Therefore it is possible to store the results of the LU decomposition using only 3 vectors each of size N.

We derive a simple and optimized algorithm that can be used to perform the LU decomposition specifically for the discretized matrix from the Implicit(2,4) scheme. The discretized matrix of the system in (21) will have the form, dropping the time dependence notation for the moment

$$\begin{bmatrix} 26 & -5 & 4 & -1 & 0 & . & 0 \\ 1 & 22 & 1 & 0 & 0 & . & 0 \\ 0 & 1 & 22 & 1 & 0 & . & 0 \\ . & . & . & . & . & . & . \\ 0 & . & . & 0 & 1 & 22 & 1 \\ 0 & . & . & -1 & 4 & -5 & 26 \end{bmatrix} \begin{bmatrix} \partial_z\zeta|_{1/2} \\ \partial_z\zeta|_{3/2} \\ \partial_z\zeta|_{5/2} \\ . \\ \partial_z\zeta|_{N-3/2} \\ \partial_z\zeta|_{N-1/2} \end{bmatrix} = \frac{24}{\Delta z} \begin{bmatrix} \zeta_1 - \zeta_0 \\ \zeta_2 - \zeta_1 \\ \zeta_3 - \zeta_2 \\ . \\ \zeta_{N-1} - \zeta_{N-2} \\ \zeta_N - \zeta_{N-1} \end{bmatrix} . \quad (22)$$

Performing one time Gauss elimination to the first and last rows only results in

$$\begin{bmatrix} 0 & 1 & 0 & 0 & 0 & . & 0 \\ 1 & 22 & 1 & 0 & 0 & . & 0 \\ 0 & 1 & 22 & 1 & 0 & . & 0 \\ . & . & . & . & . & . & . \\ 0 & . & . & 0 & 1 & 22 & 1 \\ 0 & . & . & 0 & 0 & 1 & 0 \end{bmatrix} \begin{bmatrix} \partial_z\zeta|_{1/2} \\ \partial_z\zeta|_{3/2} \\ \partial_z\zeta|_{5/2} \\ . \\ \partial_z\zeta|_{N-3/2} \\ \partial_z\zeta|_{N-1/2} \end{bmatrix} = \frac{24}{\Delta z} \begin{bmatrix} b_1 \\ \zeta_2 - \zeta_1 \\ \zeta_3 - \zeta_2 \\ . \\ \zeta_{N-1} - \zeta_{N-2} \\ b_N \end{bmatrix} \quad (23)$$

with

$$b_1 = \frac{1}{(24)^2}(27(\zeta_2 - \zeta_1) - (\zeta_3 - \zeta_0)) \quad (24)$$

and

$$b_N = \frac{1}{(24)^2}(27(\zeta_{N-2} - \zeta_{N-1}) - (\zeta_{N-3} - \zeta_N)) . \quad (25)$$

When simulating TE fields, the process of solving the linear system will be repeated twice for 1**D** problems, four times for 2**D** with PML-ABCs. For a large number of time steps, the computation time of the Implicit(2,4) scheme may limit the use of the scheme for simulating large structures. Hence, any optimization to the LU decomposition process will effectively reduce the total computation time. Rather than performing the LU decomposition on the systems in (22) or (23) as proposed in [3], we eliminate $\partial_z\zeta|_{3/2}$ and $\partial_z\zeta|_{N-3/2}$ from (23) and perform the LU decomposition. The resulting system has the form

$$\begin{bmatrix} 1 & 1 & 0 & 0 & 0 & . & 0 \\ 0 & 22 & 1 & 0 & 0 & . & 0 \\ 0 & 1 & 22 & 1 & 0 & . & 0 \\ 0 & 0 & 1 & 22 & 1 & . & 0 \\ . & . & . & . & . & . & . \\ 0 & . & 1 & 22 & 1 & 0 & 0 \\ 0 & . & 0 & 1 & 22 & 1 & 0 \\ 0 & . & 0 & 0 & 1 & 22 & 0 \\ 0 & . & 0 & 0 & 0 & 1 & 1 \end{bmatrix} \begin{bmatrix} \partial_z\zeta|_{1/2} \\ \partial_z\zeta|_{5/2} \\ \partial_z\zeta|_{7/2} \\ \partial_z\zeta|_{9/2} \\ . \\ \partial_z\zeta|_{N-9/2} \\ \partial_z\zeta|_{N-7/2} \\ \partial_z\zeta|_{N-5/2} \\ \partial_z\zeta|_{N-1/2} \end{bmatrix} = \frac{24}{\Delta z} \begin{bmatrix} b_1 \\ b_2 \\ b_3 \\ \zeta_4 - \zeta_3 \\ . \\ \zeta_{N-4} - \zeta_{N-5} \\ b_{N-2} \\ b_{N-1} \\ b_N \end{bmatrix} \quad (26)$$

with

$$b_2 = (\zeta_2 - \zeta_1) - 22b_1 \quad (27)$$

$$b_3 = (\zeta_3 - \zeta_2) - b_1 \quad (28)$$

$$b_{N-2} = (\zeta_{N-3} - \zeta_{N-2}) - b_N \quad (29)$$

$$b_{N-1} = (\zeta_{N-2} - \zeta_{N-1}) - 22b_N \quad (30)$$

The LU decomposition of the matrix in 20 will result in two matrices L and U of the following form

$$L*U = \begin{bmatrix} 1 & 0 & 0 & 0 & . & 0 & 0 \\ 0 & 1 & 0 & 0 & . & 0 & 0 \\ 0 & a_1 & 1 & 0 & . & 0 & 0 \\ 0 & 0 & a_2 & 1 & . & 0 & 0 \\ . & . & . & . & . & . & . \\ 0 & 0 & 0 & . & a_{p-1} & 1 & 0 \\ 0 & 0 & 0 & . & 0 & a_p & 1 \end{bmatrix} \begin{bmatrix} 1 & 1 & 0 & 0 & . & 0 & 0 \\ 0 & 1/a_1 & 1 & 0 & . & 0 & 0 \\ 0 & 0 & 1/a_2 & 1 & . & 0 & 0 \\ 0 & 0 & 0 & 1/a_3 & . & 0 & 0 \\ . & . & . & . & . & . & . \\ 0 & 0 & 0 & . & . & 1/a_p & . \\ 0 & 0 & 0 & 0 & . & 0 & 1 \end{bmatrix} \quad (31)$$

where p equals to N-2. The values of a_i can be calculated using the simple expression

$$a_1 = \frac{1}{22}, \quad a_i = \frac{1}{22 - a_{i-1}}, \quad i = 2,3,4,...,p. \quad (32)$$

Due to the round off error and the precision accuracy, we found that $a_i \approx a_6$ for $i \succ 6$ with error less than 10^{-15}. This suggests storing only the values $a_i,\ i = 1.2,...,6.$ This not only reduces the number of operations and the storage requirements to perform the LU decomposition but also reduces the number of operations to solve the linear system using the

above LU formulation. The algorithm used to solve the linear system $LUX = b$ will be carried out by solving $LY = b$ with $Y = UX$. For the first system the algorithm will have the form

$$Y_1 = b_1, \quad Y_2 = b_2$$
$$Y_i = b_i - a_{i-2} * Y_{i-1} \qquad i = 3,4,5,....,p+2 \quad (33)$$

and for solving $Y = UX$

$$X_{p+2} = Y_{p+2}, \qquad X_{p+1} = Y_{p+1} * a_p$$
$$X_i = (Y_i - X_{i+1}) * a_{i-1}, \quad i = p-1, p-2, ..., 2$$
$$X_1 = Y_1 - X_2. \quad (34)$$

2.3 Accuracy of Different FDTD Schemes

We confirm the second and fourth order of accuracy with respect to the spatial discretization of the previously presented FDTD schemes in one dimension, similarly the extension in two dimensions. The results shown in Figure 2 are obtained for a sinusoidal wave with wavelength $1.0\mu m$ propagating in free space in the positive $z-$ direction over a distance of $10\mu m$, where N is the number of discretization points. For $\varepsilon_r = 1$, angular frequency ω, and wavenumber k, an exact solution of the 1**D** TE field equations can be found.

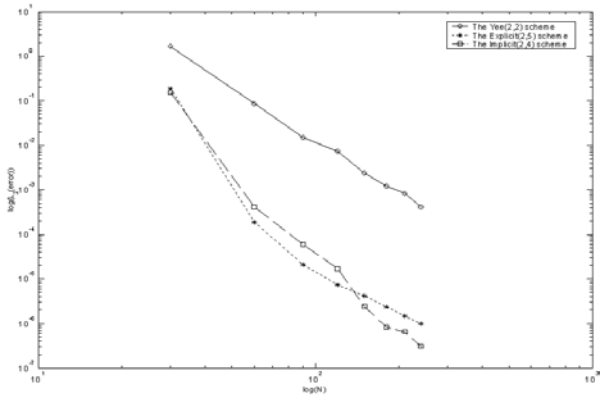

Fig. 2. L_2 norm of the difference between the numerical and exact values for E_y field at the last time step using the Yee(2,2), Explicit(2,4), and Implicit(2,4) scheme at different points per wavelength.

3. One-Sided Total-Field/Scattered-Field Formulation

The total-field/scattered-field (TF/SF) technique [5] is an efficient way to increase the quality of simulations through reducing the load on the ABCs and by offering information about scattered fields. The TF/SF was originally proposed for free space problems and for modeling point sources, which are not of great practical interest in integrated optics problems.

The simulation domain is divided into three domains: the total-field domain, the scattered field domain, and the PML domain, as in Figure 3. The formulation is based on the linearity of the Maxwell equations and on decomposing the electric and magnetic fields as sum of two components, one in the total field region and another in the scattered field region

$$E_t = E_i + E_s, \quad (35)$$
$$H_t = H_i + H_s, \quad (36)$$

where ξ_i is the incident field value, ξ_s is the scattered field value, and ξ_t is the total field value, $\xi = \{E, H\}$.

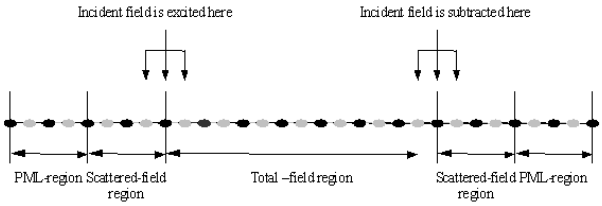

Fig. 3. The FDTD regions for 1D TF/SF grid.

Consider the 1**D** mesh as shown in Fig. 3 where two scattered-field regions are defined on both ends of the simulation domain. We call this formulation two-sided TF/SF formulation. In most of the structures of interest to our work the amount of scattering on the right side of the simulation domain is much less compared to the left side and therefore no scattered field region is added on the right side of the simulation domain. We refer to such formulation the one-sided TF/SF formulation.

The black dots in Fig. 4 are the positions of the electric field E_y, and the gray dots are the positions of the magnetic field H_x. In the total-field region, the FDTD algorithm is applied to the total field, while in the scattered-field region it is applied to scattered field only. On the interface between these two regions the incident field is

taken into account. Details of these formulation in 1**D**, 2**D**, and 3**D** are well documented in [5]. For the 1**D** TE Yee(2,2) scheme, only two FDTD update equations need modification. The first for the E_y field update equation at the TF-SF interface and the second for the H_x field update equation at the first point to the left to the TF-SF interface [5].

The discretization equations of the FDTD scheme with one-sided TF/SF formulation for 2**D** structures are similar to those introduced in [5] with one difference that is simply having no scattered field region at the right side of the simulation domain, see Fig. 4(a). As described in [5] the incident fields at all time steps need to be known for regions around the total-field – scattered-field interfaces. These fields are obtained from a separate simulation and are used as incident fields in the same regions. If the same incident fields are used to excite different structures then these fields can be stored and used in these simulations. Otherwise two simulations are run simultaneously, one for calculating the incident fields and are used as the incident fields in the same regions in the second simulation. Running two simulations approximately doubles both the memory and computational time requirements compared to running a single simulation and using stored values of the incident fields in the incident field regions. For our work the two simulation approach was selected and implemented for arbitrarily choosing the incident structures, the incident propagating mode, the simulation window etc.

Figs. 4(a) and 4(b) show the domains of the two FDTD simulations that run simultaneously. In the first simulation, the waveguide that is used to excite the structure in 4(a) is extended to the right hand side of the FDTD domain, see Fig. 4 (b). The waveguide is excited by incident modal field using the hard source excitation (the modal profile of the propagating mode of interest is obtained from a separate mode solver program, the width and refractive indices of both the exciting waveguide and background are inputs to this mode solver). Hard source excitation has the advantage of coupling the exact power into the FDTD grid compared to other excitations [2], [4].

In the second simulation with the configuration shown in Fig. 4 (a), at each time step fields obtained from the first simulation at the incident field regions are used to introduce the incident field in the same regions. For most of our simulations the size, number of cells, of the scattered-field region was equal to those of the PML region.

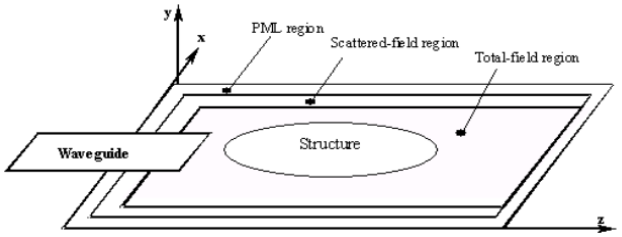

(a)

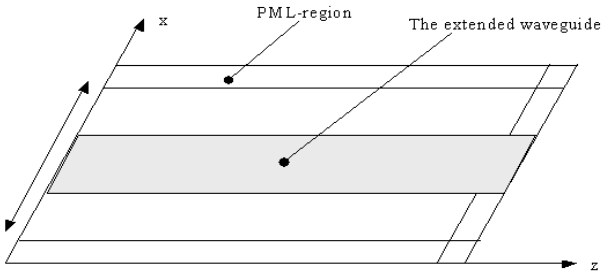

(b)

Fig. 4. (a) 2D one sided-TF/SF problem geometry, (b) 2D-problem domain for simulation of the incident field in the absence of any structures inside the TF region.

The following example demonstrates how the developed FDTD scheme with the one-sided TF/SF formulation works. Fig. 5 (b) shows the intensity plot of the E_y field for TE polarization for the cos-bend waveguide sketched in Fig. 5 (a), with width $0.5\ \mu m$, length $10\ \mu m$, offset $2\ \mu m$, and $d\alpha$ $0.1\ \mu m$. At the plane in and plane out positions the cos-bend is connected to a waveguide with the same width of the cos-bend and a length $2\ \mu m$. The refractive index of the background is 1.0 and a refractive index of 3.0 in the guiding regions. No special treatment was applied to dielectric interfaces and structures with magnetic material were not considered in this work.

The computational window is $5\times15\ \mu m$ in the x- and z-directions, and the wavelength is $1.5\ \mu m$, Δz and Δx were chosen to be $0.05\ \mu m$ and simulation is performed for $300\ fs$ with dt equal to $0.05\ fs$. The values for the PML parameters are 8, 3, 10 for the number of PMLs cells, the polynomial degree of the conductivity profile, and the reflectivity, respectively, in both the z- and x-directions. Fig. 5

(c) shows the intensity of the incident field propagating in the extended waveguide.

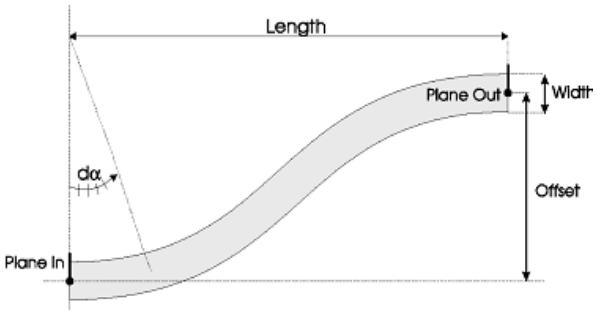

(a)

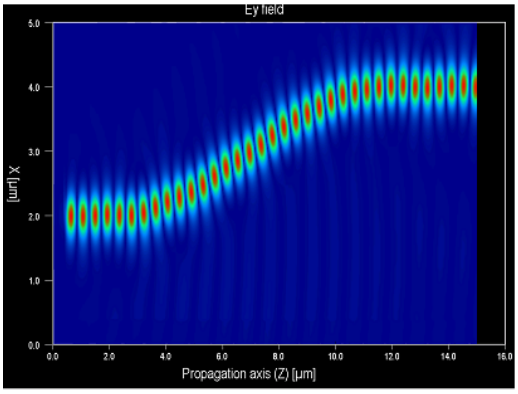

(b)

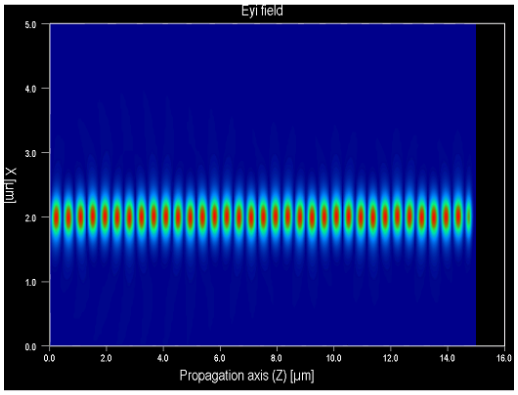

(c)

Fig. 5. (a) cos-bend waveguide, (b) the intensity of the E_y field in the SF region, (c) The intensity plot of TE-E_y field propagating in an extended waveguide used in the TF/SF excitation.

The developed simulation tool was integrated into the Prometheus program, a software package of Kymata Netherlands company (currently C2V) [6]. Prometheus is a design, simulation and mask layout platform for integrated optics devices.

Two examples are presented here to validate the accuracy of the developed simulation tool. In the first example a straight waveguide is excited by the modal filed of the fundamental mode and the overlap coefficient between the input field and the output field at the end of the waveguide is calculated. All the temporal field values of the E_y component for both the input and output field are stored. Then they are Fourier transformed and the overlap is calculated. The overlap coefficient for a waveguide with parameters $1.55\mu m$, $3\mu m$, $1\mu m$, $5\mu m$, $5\mu m$ for the wavelength, the refractive index of the waveguide, the background refractive index, the x-section and z-section of the computational window, respectively, is found to be 0.996. Figure 6 shows the plot of the normalized amplitude of the input and output field of the waveguide.

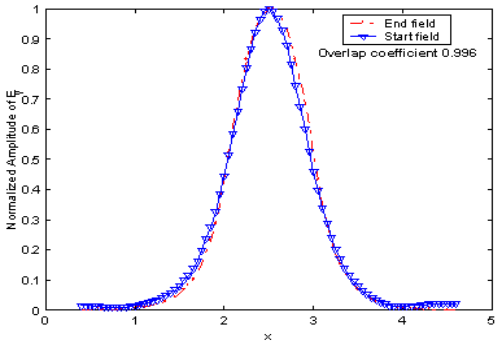

Fig. 6. Start and end field of a waveguide simulation.

The second example that validates the accuracy of the developed simulation tool is a directional coupler was modeled using the Prometheus program and the developed simulation tool. Figure 7 (a) shows the intensity plot of the E_y field for a directional coupler of length 75 μm, this is also the length of the computational window, widths of the waveguides are 1 μm and core separation is 1 μm. Figure 7(b) shows the intensity plot of E_y field calculated using Prometheus program of Kymata software.

The wavelength was 5 μm, smaller wavelengths require long waveguides which means a huge number of grid points, and the width of the computational window in the x-direction was 10 μm. The step size was 0.1 and 0.25 μm in the x- and z-directions, respectively. The coupling length calculated using the Prometheus program 20.6303 μm while the one calculated using the developed simulation tool is 20.62143 μm.

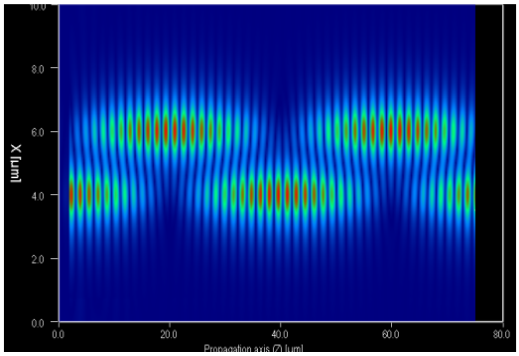

(a)

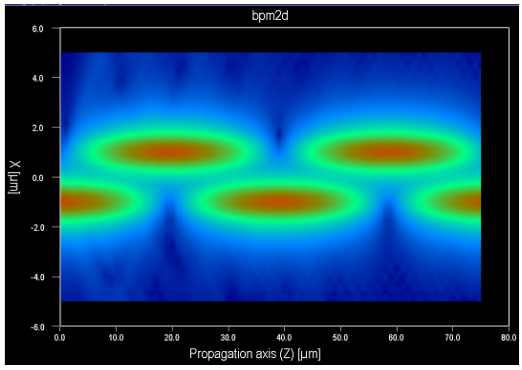

(b)

Fig. 7. The intensity plot of the E_y field component for a directional coupler, (a) calculated using the FDTD method, (b) calculated using the Prometheus software program of Kymata Netherlands.

The results presented in the previous two examples show that the accuracy of the developed simulation tool is in good agreement with the accuracy of the Prometheus program, a widely accepted software package in the integrated optics community.

4. Conclusions

An optimized implicit high-order finite difference time domain (FDTD) solver with one-sided total-field/scattered field formulation for time dependent numerical simulation of integrated optical components is developed and its accuracy was verified versus results calculated by the Prometheus program. A reduced LU decomposition was developed for inverting matrices that arise from the implicit FDTD scheme. Although implicit high -order FDTD schemes are unconditional stable, implementing them seem to be feasible only for 1D or 2D problems due to the increasing computational cost compared to explicit schemes.

5. References

[1] Kane S. Yee, "Numerical solution of initial boundary value problems involving Maxwell's equations in isotropic media", IEEE Trasaction on Antennas and Propagation, vol. Vol. AP-14, No. 3, pp. 302–307, 1966.

[2] H.A. AbdAllah,"General purpose numerical schemes for simulating light propagation in photonic structures", Literature Study Report, part of course work for MSc in Engineering Mathematics, University of Twente, 2001.

[3] A.Yefet and E. Turkel, "Fourth order compact implicit method for the Maxwell equations", Applied Numerical Mathematics, vol. 33, pp. 125–134, 2000.

[4] H. A. AbdAllah, "Simple Dispersion Analysis of 2nd and 4th order FDTD Schemes", The Annual Review of Progress in Applied Computational Electromagnetics Conference, Syracuse NY, 2004

[5] A.Ta‡ove, Computational Electrodynamics: The Finite Difference Time Domain Methods, Artech House, MA, Boston, 1995.

[6] Kymata Prometheus, Kymata Netherlands, Enschede, The Netherlands, 2001. www.kymata.nl (currently, www.c2v.nl)

Acknowledgment

The author would like to acknowledge the valuable discussion and comments from Manfred Hammer, Twente University, Enschede-The Netherlands and Jan Bos, Kymata Netherlands, Enschede-The Netherlands

Hossam A. Abdallah was born in Alexandria, Egypt, in 1973. He received his Bachelor of Science degree in computer science in 1995 from Alexandria University, Alexandria, Egypt. In 2001 he received his MSc degree in Engineering Mathematics from Twente University, Enschede, The Netherlands. Since August 2001, Mr. Abdallah is pursuing his PhD degree in the area of array signal processing and also working as a research assistant at the department of electrical and computer engineering, The George Washington University, Washington DC, USA. His current research activities are computational electromagnetics and array signal processing.